Korean J. Chem. Eng., 33(1), 57-62 (2016)
DOI: 10.1007/s11814-015-0037-7

pISSN: 0256-1115
eISSN: 1975-7220

Microfluidic room temperature ionic liquid droplet generation depending on the hydrophobicity and interfacial tension

Jung Wook Hwang*, Joo-Hyung Choi, Bumjoon Choi***, Gyudo Lee***, Sang Woo Lee***, Yoon-Mo Koo**, and Woo-Jin Chang*,†**

*Department of Mechanical Engineering, University of Wisconsin-Milwaukee, 3200 N Cramer Street, Milwaukee, WI 53211, USA
**Department of Biological Engineering, 253 Yonghyun-dong, Nam-gu, Incheon 402-751, Korea
***Department of Biomedical Engineering, Yonsei University, 1 Yonseidae-gil, Wonju, Gangwondo 220-710, Korea
(*Received 24 June 2014 • accepted 16 February 2015*)

Abstract−We have characterized micro-droplet generation using water immiscible hexafluorophosphate ([PF_6])- and bis(trifluoromethylsulfonyl)imide ([Tf_2N])-based room temperature ionic liquids (RTILs). The interfacial tension between total 7 RTILs and phosphate buffered saline (PBS) was measured using a tensiometer for the first time. PBS is one of the most commonly used buffer solutions in cell-related researches. The measured interfacial tension ranges from 8.51 to 11.62 and from 9.56 to 13.19 for [Tf_2N]- and [PF_6]-based RTILs, respectively. The RTILs micro-droplets were generated in a microfluidic device. The micro-droplet size and generation frequency were determined based on continuous monitoring of light transmittance at the interface in microchannel. The size of RTIL micro-droplets was inversely proportional to the increase of PBS solution flow rate and RTILs hydrophobicity, while droplet generation frequency was proportional to those changes. The measured size of RTILs droplets ranged from 0.6 to 10.5 nl, and from 1.0 to 17.1 nl for [Tf_2N]- and [PF_6]-based RTILs, respectively. The measured frequency of generated RTILs droplets ranged from 2.3 to 37.2 droplet/min, and from 2.7 to 17.1 droplet/min for [Tf_2N]- and [PF_6]-based RTILs, respectively. The capillary numbers were calculated depending on the RTILs, and ranged from 0.51×10^{-3} to 1.06×10^{-3} and from 5.00×10^{-3} to 8.65×10^{-3}, for [Tf_2N]- and [PF_6]-based RTILs, respectively. The interfacial tension between RTILs and PBS will contribute to developing bioprocesses using immiscible RTILs. Also, the RTILs micro-droplets will enable the high-throughput monitoring of various biological and chemical reactions using RTILs as new reaction media.

Keywords: Interfacial Tension, Light Transmittance, Micro-droplet, Microfluidic Device, Water Immiscible Room Temperature Ionic Liquids (RTILs)

INTRODUCTION

RTILs, which are organic salts melted below 100 °C [1,2], have received great interest as green solvents due to non-volatility and thermal stability. An enormous number of different RTILs with different chemical and physical properties, such as viscosity, polarity, hydrophobicity, and water miscibility are available by the combination of various anions and cations [3,4]. Furthermore, chemical and biological reactions can occur with excellent activity, selectivity, and stability [5] inside RTILs. RTILs that are insoluble not only in water but also in organic solvents can be synthesized as well [6]. Thus, various combinations, such as aqueous solution-RTILs, organic solvent-RTILs, RTILs-RTILs, can supply huge number of different bi- or multi-phasic systems for various biological and chemical reactions.

Micro-droplets have obtained increasing interest as nanoliter-scale reactors in high-throughput screening of various chemical and biological reactions recent years [7,8]. Reported applications using micro-droplets include analysis of DNA [9], characterization of proteins crystallization [10], formation of polymeric beads [11,12], measurement of enzyme kinetics [13,14] etc. Microfluidic device enables the generation of massive number of controllable-size monodispersed droplets. Thus, various channel designs and theoretical analysis has been suggested regarding the micro-droplet generation in microfluidic devices [15-17]. Water immiscible liquids such as oil [18], hydrocarbon and organic solvents [19] have been used for the formation of micro-droplets in a microchannel. However, novel water-immiscible solvents having various physical and chemical properties and low vapor pressure are required to overcome lack of solvent polarity, toxicity on biomolecules, and device deformation, possibly caused by conventionally used water immiscible fluids [20]. Thus, micro-droplet technology using water immiscible RTILs is promising for high-throughput screening of biological and chemical reactions. Also, this method can be used to select RTIL appropriate for specific reaction.

Recently, ionic liquid such as [BMIM][BF_4] and [BMIM][PF_6] have been used for droplet-based microfluidic devices [21]. Joule heating of ionic liquids has been suggested to make controllable temperatures in microfluidic devices [22]. Reported electrochemical and biological applications using RTILs include electroanalyti-

†To whom correspondence should be addressed.
E-mail: wjchang@uwm.edu

cal sensors and gas analysis in medium [23]. The RTILs were also used for the monitoring of live cardiomyocyte culture in PDMS micro well [24].

In this study, the formation of water-immiscible RTILs micro-droplet in a PDMS-based microfluidic device was investigated. The visible light transmittance was optically measured to determine the size and frequency of generated RTIL micro-droplets. The size and frequency of micro-droplets is determined as a function of the flow rate ratio of PBS and RTILs and hydrophobicity of RTILs. [Tf_2N]- and [PF_6]-based RTILs that have different hydrophobicities were used. The interfacial tension between PBS and RTILs was also measured and correlated to the micro-droplet formation characteristics.

EXPERIMENTAL

1. Microfluidic Device Fabrication

A PDMS (Sylgard 184, Dow Corning, USA) microfluidic device shown in Fig. 1(d) was prepared by soft lithographic fabrication process [25]. Briefly, the master mold for the replica molding of the PDMS device was fabricated on a silicon wafer using an SU-8 negative photoresist (Microchem, USA) and the photo-mask. The surface of the master mold was functionalized with trichloro(3,3,3-trifluoropropyl) silane (Sigma-Aldrich, USA) for stripping the hardened PDMS easily after molding at 55 °C for 8 h. The surface of the molded PDMS was treated by a plasma generator (Electro-Technic Products, USA) and then attached onto another PDMS layer for permanent bonding. Subsequently, Silastic™ silicone tubing (Dow Corning, USA) was bonded through a punched hole in the PDMS layer and used for the injection of the solutions. The dimension of microfluidic device is indicated in Fig. 1(d). The height of the microchannel was 52 μm.

2. Micro-droplets Generation

Micro-droplets were formed with PBS (pH 7.0) and water immiscible RTILs in the microfluidic device. Each fluid was injected using a 50 μl micro-syringe (ILS, Germany) and a 250I syringe pump (World Precision Instrument, USA). The size and frequency of the generated micro-droplets were measured using a BX51 fluorescence microscope (Olympus, Japan) equipped with photomultiplier tube (PMT, Hamamatsu H7467, Japan). The images were obtained by DP-70 cooled-CCD camera (Olympus, Japan).

A schematic drawing (Fig. 1(a)), photograph of the experimental setup (Fig. 1(b)) and dimensions are shown in Fig. 1. Micro-droplets were generated at the cross junction region of microchannel in which RTIL and two PBS buffer streams encountered each other. RTIL was introduced through the horizontal microchannel while two PBS buffers were infused from two vertical channels. Water immiscible RTILs with different hydrophobicities were used. Those are 1-ethyl-3-methylimidazolium bis(trifluoromethylsulfonyl)imide ([EMIM][Tf_2N])), 1-butyl-3-methylimidazolium bis(trifluoromethylsulfonyl)imide ([BMIM][Tf_2N]), 1-hexyl-3-methylimidazolium bis(trifluoromethylsulfonyl)imide ([HMIM][Tf_2N]), 1-octyl-3-methylimidazolium bis(trifluoromethylsulfonyl)imide ([OMIM][Tf_2N]), 1-butyl-3-methylimidazolium hexafluorophosphate ([BMIM][PF_6]), 1-hexyl-3-methylimidazolium hexafluorophosphate ([HMIM][PF_6]), and 1-octyl-3-methylimidazolium hexafluorophosphate ([OMIM][PF_6]) (C-Tri Co., Korea). The flow rate of the RTIL was fixed as 0.03 μl/min, while the injection ratio was varied from 1 : 1 : 1 to 4.5 : 1 : 4.5 by changing flow rate of PBS. Consequently, the total flow rate was increased from 0.09 to 0.3 μl/min, depending on the flow rates of PBS.

3. Interfacial Tension Measurement

A small quantity of residual water in RTILs was removed before use in a desiccator with molecular sieve more than 12 hours. A bipha-

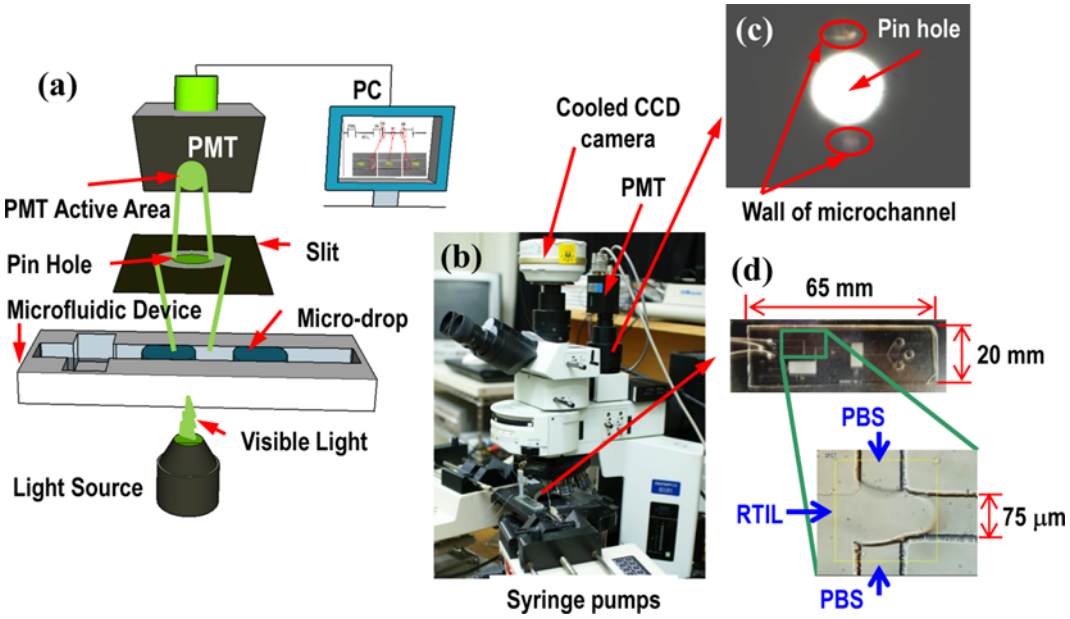

Fig. 1. Experimental setup and dimension of the microfluidic device. (a) Schematic drawing of the visible light transmittance monitoring to determine droplet size (drawn not to scale), (b) optical micrograph of experimental set-up, (c) picture of the actual area used for the measurement of light transmittance, (d) cross-junction to generate micro-droplet.

sic solution having 10 ml of RTIL and PBS each was kept in a shaking incubator at 25 °C and 180 rpm for five days to reach equilibrium, and then allowed to settle down without shaking for 1 day before measurement. RTILs form the bottom phase due to higher density than PBS. Interfacial tension between RTILs and PBS was measured with a Surface Tensiomat® 21 (Fisher Scientific, USA) equipped with platinum wire ring (diameter 1 cm). The platinum wire ring was submerged in the middle of the bottom RTILs phase, and then moved upward to the middle of thte top PBS phase. The interfacial tension was measured when the platinum wire ring passes through the interface between RTILs and PBS.

4. Micro-droplet Size Measurement

The size and number of micro-droplets were calculated from the measured data with the photon-counting PMT mounted on a microscope. A slit with a 2 mm diameter pin-hole at the center was positioned in front of the PMT to restrict the area to measure the amount of transmitting light. Since the pin-hole covered the side walls of the microchannel, the amount of light only passing through the inside of the microchannel was measured (Fig. 1(c)). The transmitting light through the microchannel was scattered at the interface between RTIL and PBS. Thus, the number of measured photons decreased rapidly when the interface between RTILs and PBS passed under the observation area (Fig. 2). The time interval between two passing interfaces was converted into the volume of the RTIL micro-droplet using microchannel dimension and the total volumetric flow rate of the liquids. Similarly, the volume of PBS between two RTIL droplets was determined. The RTIL droplet generation frequency was calculated using time interval for one RTIL and one PBS droplet as a repeating unit.

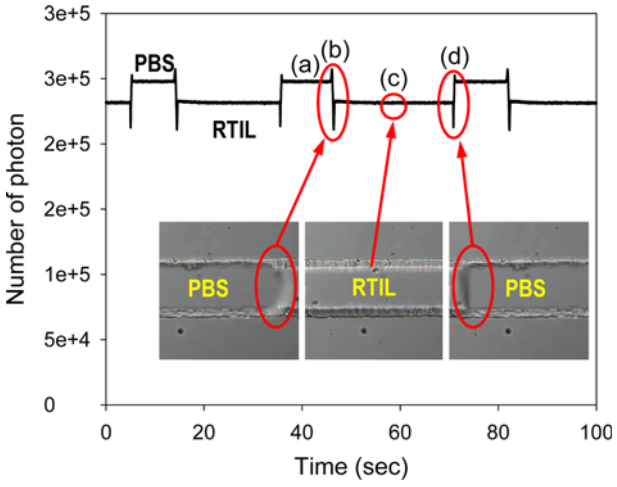

Fig. 2. Optical micrograph and measured transmittance (number of photon) during droplet generation. (a) PBS phase, (b) RTIL to PBS interface, (c) RTIL phase, and (d) PBS to RTIL interface.

RESULTS AND DISCUSSION

1. Interfacial Tension between RTILs and PBS Solution

RTILs can have various chemical and physical properties depending upon the combination of cation and anion. Some reported important physical and chemical characteristics of RTILs used in this study are summarized in Table 1 [26-28]. Log P in Table 1, which is calculated from the dissolved concentration ratio of RTIL in water/octanol two-phase system, represents the hydrophobicity of the molecule. The hydrophobicity of RTILs increases as increasing the alkyl chain length. The preferred phase of RTIL is inverted from water to octanol when the number of carbon atoms in the alkyl chain bound to the cation is increased from 4 ([BMIM]) to 6 ([HMIM]) in both of [Tf_2N]- and [PF_6]-based RTILs. On the other hand, [PF_6]-based RTILs have higher solubility in water than [Tf_2N]-based RTILs. These differences are coming from the hydrophobicity difference between anions. The anion, [Tf_2N], is more hydrophobic than [PF_6]. The viscosity is increased from 6.8 to 10.2 times among tested RTILs when anion, [Tf_2N] is replaced with [PF_6], which affects the characteristics of the micro-droplet generation as well. The [EMIM][PF_6] is not included in the table, since it is miscible with water at room temperature. However, the measured properties have large variation, depending on the measurement condition. Thus, a more accurate method is required to obtain physical and chemical properties of the RTILs.

The interfacial tension between RTILs and PBS, which is an important parameter to determine the size and frequency of micro-droplet generated in the microchannel, was measured and displayed in Table 2. Even though information on the properties of an interface between RTIL and an aqueous solution is essential to give insight of the surface activity of RTILs, the thermodynamics and kinetics of extraction, and mass or charge transfer at the interfaces, only a few results on the interfacial tension between water and immiscible RTILs are reported so far [30]. According to our investigation on the interfacial tension between RTIL and PBS, RTILs that have the same alkyl chain length show similar interfacial tension. For example, the interfacial tension of the RTILs that have [HMIM] is

Table 1. Selected properties of [Tf_2N]- and [PF_6]-based RTILs used in this study

	Log P	Molecular weight (g/mol)	Density (g/cm^3)	Viscosity (cp)	Solubility in water (%, w/w)
[EMIM][Tf_2N]	−1.18	391.3	1.519	28-34	1.9
[BMIM][Tf_2N]	−0.55	419.4	1.436	52-53	1.5
[HMIM][Tf_2N]	0.16	447.4	1.373	59-68	1.1
[OMIM][Tf_2N]	0.79	475.5	1.317	93	0.9
[BMIM][PF_6]	−2.39	284.2	1.373	389	3.1
[HMIM][PF_6]	0.23	312.2	1.304	688	2.4
[OMIM][PF_6]	0.45	340.3	1.235	691	1.8

Table 2. Measured interfacial tension between PBS and [Tf_2N]- and [PF_6]-based RTILs, and calculated capillary number in droplet generation

	Interfacial tension (dyn/cm)	Capillary number ($\times10^{-3}$)
[EMIM][Tf_2N]	8.51±1.74	0.191
[BMIM][Tf_2N]	10.52±2.68	0.249
[HMIM][Tf_2N]	13.76±1.38	0.254
[OMIM][Tf_2N]	11.62±2.59	0.400
[BMIM][PF_6]	9.56±1.04	1.880
[HMIM][PF_6]	13.19±0.51	2.480
[OMIM][PF_6]	11.98±1.37	3.251

13.76 with [Tf_2N] and 13.16 with [PF_6]. Overall, the interfacial tension is increasing with the increased alkyl chain length bound to the cation until 6 ([HMIM]) in both RTIL groups (Table 2). On the contrary, the interfacial tension is decreasing when the chain length is 8 ([OMIM][Tf_2N] and [OMIM][PF_6]). Fitchett et al. [30] reported that the interfacial tension in a water-immiscible RTILs biphasic reaction system containing bis(perfluorethysulfonyl)imide (BETI) or bis(perfluoromethylsulfonyl)imide (BMSI) anion with 0.1 M LiCl solution decreased according to the increase of alkyl chain length on cation from 6 to 12 [30]. Interestingly, it is opposite to the air-RTILs systems where interfacial tensions increased with longer alkyl chain. In our case, the measured interfacial tension decreased with [OMIM], even though the hydrophobicity and alkyl chain length was increased. A higher hydrophobicity in [OMIM]-based RTILs is supposed to stimulate RTIL aggregation, and thus the interfacial tension with aqueous solution was decreased, similar to previously reported BETI- and BMSI-based RTILs. However, further investigation is needed to completely understand these interfacial tension issues in [OMIM]-based RTILs.

2. Optical Detection of RTIL Micro-droplets

RTIL injected through the middle channel was pinched and chopped by two PBS solutions, as shown in Fig. 1(d), and this is resulted in the formation of RTIL micro-droplet. The different visible light transmittance in RTIL and PBS liquids enables the optical detection of the RTIL droplet. The transmittance of visible range light in RTIL was approximately 10% lower than PBS (Fig. 2(a) and (c)). Therefore, the detected number of photons was abruptly changed when the front (Fig. 2(d)) and the end (Fig. 2(b)) of the interface between RTIL and buffer solution passed under the monitored area. Rapid drop of the number of transmitting photons occurred by scattering the light at the interface. The distance between those peaks generated from the interfaces are corresponding to the length of each RTIL micro-droplet, as well as PBS spacer.

3. Characteristics of Micro-droplets Generation

The size of RTIL micro-droplet was inversely proportional to the hydrophobicity of RTILs, as well as PBS flow rate, except for [OMIM][Tf_2N] (Fig. 3(a)). The volume of generated [EMIM][Tf_2N] micro-droplets, which has minimum hydrophobicity among the tested [Tf_2N]-based RTILs, dramatically decreased from around 11 to 2 nl. On the other hand, the most hydrophobic [OMIM][Tf_2N] did not be matched in this trend; instead, similar size micro-droplets were generated with 4.5 : 1 : 4.5 and 2.5 : 1 : 2.5 ratios. The viscosity and interaction between RTIL and the microchannel wall should affect the size of micro-droplet. Higher viscosity and hydrophobicity of [OMIM][Tf_2N] would be expected to make the RTIL capable of resist the shear force between PBS and RTIL, which cut the RTIL phase into small micro-droplet. Stronger interaction between hydrophobic surface of PDMS and hydrophobic RTIL could enhance this as well. Choi et al. [29] showed the microchannel wall that has lower wettability (more hydrophobic) makes smaller water droplets; however, further investigation on the properties of the channel surface and the size of RTILs micro-droplet is needed to explain this phenomenon more accurately.

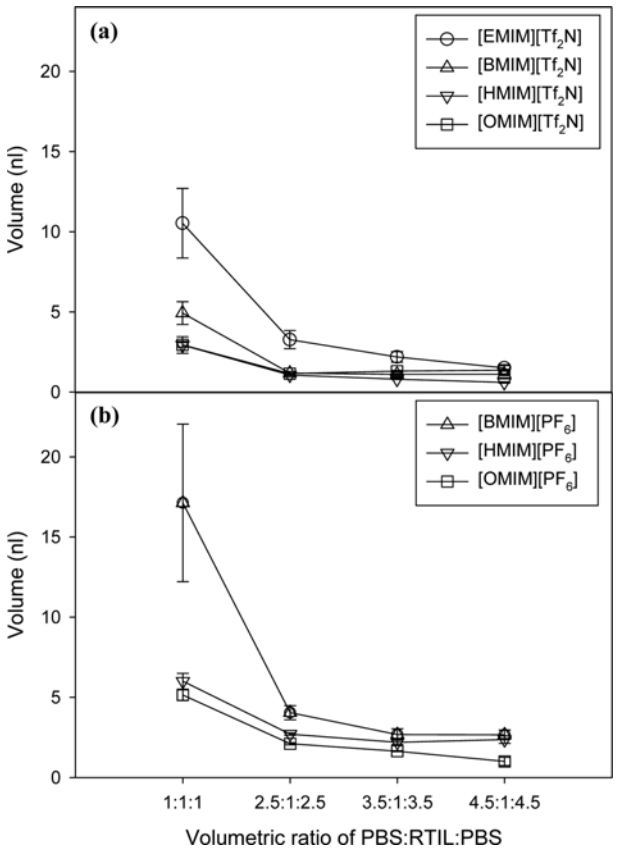

Fig. 3. Volume of generated RTIL micro-droplets with volumetric injection ratio of PBS, RTIL and PBS. (a) [Tf_2N]-based RTILs, (b) [PF_6]-based RTILs.

The [PF_6]-based RTILs show similar characteristics with [Tf_2N]-based RTILs as shown in Fig. 3(b). However, the volume of generated micro-droplets are larger than [Tf_2N]-based RTILs. Considering higher viscosity and lower hydrophobicity of [PF_6]-based RTILs than [Tf_2N]-based RTILs, the viscosity affects the droplet size more than hydrophobicity.

The droplet generation frequencies using [Tf_2N]- and [PF_6]-based RTILs are displayed in Fig. 4, respectively. The [Tf_2N]-based RTILs have higher droplet generation frequency (ranged from 2.3 to 37.2 droplet/min) than [PF_6]-based RTILs (ranged from 2.7 to 17.1 droplet/min). In general, the frequency is higher with the RTIL and fluidic condition to generate smaller droplet. For example, the RTIL generated smallest droplets, i.e., [HMIM][Tf_2N], shows highest fre-

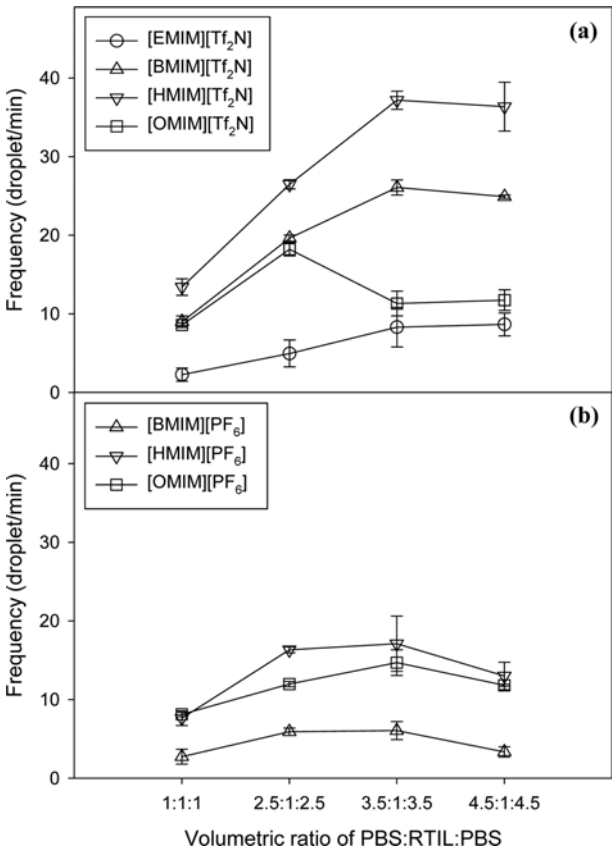

Fig. 4. Frequency of generated RTIL micro-droplets with volumetric injection ratio of PBS, RTIL and PBS. (a) [Tf_2N]-based RTILs, (b) [PF_6]-based RTILs.

quency of droplet generation among tested RTILs as shown in Fig. 4(a). The RTILs generated larger droplets, i.e., [EMIM][Tf_2N] and [BMIM][PF_6], show lowest generation frequency (Fig. 4(a) and (b)). As shown in Fig. 3, the sizes of generated [HMIM]- and [OMIM]-based RTILs droplets are similar when the volumetric flow ratio of the PBS : RTIL : PBS is larger than 2.5 : 1 : 2.5. However, droplet generation frequency of [OMIM]-based RTILs is lower than [HMIM]-based RTILs in both [Tf_2N]- and [PF_6]-based RTILs. Interestingly, the frequency with highest volumetric flow ratio, i.e., 4.5 : 1 : 4.5, is not significantly higher than 3.5 : 1 : 3.5. Considering the instability of the flow with the ratio higher than 4.5 : 1 : 4.5, the maximum frequency is expected to be around 40 and 20 droplet/min for [Tf_2N]- and [PF_6]-based RTILs, respectively.

Table 2 also shows the calculated capillary number of RTILs droplet generation based upon the measured interfacial tension between RTIL and PBS. Capillary number is a ratio between viscous and capillary force, and it is often used to show the characteristics of the droplet formation, for example stable droplet generation range, not only in a micro-channel or capillary but also in membrane emulsification [31]. Capillary number, Ca, which is defined as $Ca = \mu U/\sigma$, where μ is the viscosity of the constant phase (RTIL in this study), U is the linear flow rate of the constant phase, and σ is the interfacial tension between the two phases. The linear flow rate of the constant phase was 0.05×10^{-6} m/s in this study. More hydrophobic RTILs exhibited larger Ca, and ranged from 0.191×10^{-3} to 0.400×10^{-3} and from 1.880×10^{-3} to 3.251×10^{-3} for [Tf_2N]- and [PF_6]-based RTILs, respectively. The [PF_6]-based RTILs have higher Ca due to higher viscosity. Interestingly, the Ca of both [OMIM]-based RTILs was increased compared with [HMIM]-based RTILs, while interfacial tensions of those RTILs were decreased. The increased Ca in [OMIM]-based RTILs originates from the larger viscosity and smaller interfacial tension. The Ca in [PF_6]-based RTILs is larger than [Tf_2N]-based RTILs, because of around ten-times larger viscosity. The Ca in RTILs is much smaller than that of conventional Ca between oil and water, which means the more difficult detachment of the RTILs droplet than oil [32]. Consequently, larger RTILs micro-droplets are formed. Thus, the further addition of physical assistant method, such as ultrasonic vibration, local heating, or geometrical modification, may be required to generate smaller RTILs micro-droplets with higher frequency.

CONCLUSIONS

The RTIL micro-droplet generation in a microfluidic device was characterized. The size and frequency of the generated micro-droplet was measured using optical method with visible light transmittance and a conventional microscope. The higher viscosity and hydrophobicity of the RTILs make larger micro-droplets than oil. The lower capillary number in RTIL micro-droplets generation condition than that of oil verifies this as well. The characteristics of the RTILs micro-droplet generation will enhance the application of RTILs as a novel nanoliter-scale reactor in microfluidic device by using various physical and chemical properties of RTILs. High-throughput screening of appropriate RTILs using developed technique can expand the application of RTILs in various chemical and biological reactions as a green solvent.

ACKNOWLEDGEMENTS

This material is based upon work supported by the National Science Foundation under Grant No. ECCS-1201885.

REFERENCES

1. S. H. Lee, S. H. Ha, N. M. Hiep, W. J. Chang and Y. M. Koo, *J. Biotechnol.*, **133**, 486 (2008).
2. G. Yassaghi, A. Davoodnia, S. Allameh, Z. B. Atefeh and T. H. Niloofar, *Bull. Korean Chem. Soc.*, **33**, 2724 (2012).
3. Y. H. Moon, S. M. Lee, S. H. Ha and Y. M. Koo, *Korean J. Chem. Eng.*, **23**, 247 (2006).
4. H. V. R. Annapureddy and L. X. Dang, *J. Phys. Chem. B*, **117**, 8555 (2013).
5. S. H. Lee, T. T. N. Doan, S. H. Ha, W. J. Chang and Y. M. Koo, *J. Molec. Catal. B: Enz.*, **47**, 129 (2007).
6. J. K. Lee and M. J. Kim, *J. Org. Chem.*, **67**, 6845 (2002).
7. D. Belder, *Angew. Chem. Int. Ed.*, **44**, 3521 (2005).
8. K. S. Krishna, Y. Li, S. Li and C. S. S. R. Kumar, *Adv. Drug Deliv. Rev.*, **65**, 1470 (2013).
9. Y. Zhang, V. Bailey, C. M. Puleo, H. Easwaran, E. Griffiths, J. G. Herman, S. B. Baylin and T. H. Wang, *Lab Chip*, **9**, 1059 (2009).
10. L. Chen, L. Li, S. Reyes, D. N. Adamson and R. F. Ismagilov, *Lang-*

muir, **23**, 2255 (2007).
11. T. Nisisako, T. Torii and T. Higuchi, *Chem. Eng. J.*, **101**, 23 (2004).
12. K. Aketagawa, H. Hirama and T. Torii, *J. Mater. Sci. Chem. Eng.*, **1**, 1 (2013).
13. H. Song and R. F. Ismagilov, *J. Am. Chem. Soc.*, **125**, 14613 (2003).
14. S. L. Sjostrom, H. N. Joensson and H. A. Svahn, *Lab Chip*, **13**, 1754 (2013).
15. T. Thorsen, R. W. Roberts, F. H. Amold and S. R. Quake, *Phys. Rev. Lett.*, **86**, 4163 (2001).
16. R. Dreyfus, P. Tabeling and H. Willaime, *Phys. Rev. Lett.*, **90**, 144505 (2003).
17. C. X. Zhao, *Adv. Drug Deliv. Rev.*, **65**, 1420 (2013).
18. F. Courtois, L. F. Olguin, G. Whyte, D. Bratton, W. T. S. Huck, C. Abell and F. Hollfelder, *Chem. BioChem.*, **9**, 439 (2008).
19. Z. T. Cygan, J. T. Cabral, K. L. Beers and E. J. Amis, *Langmuir*, **21**, 3629 (2005).
20. J. Lee, M. J. Kim and H. H. Lee, *Langmuir*, **22**, 2090 (2006).
21. D. D. Chatterjee, B. Hetayothin, A. R. Wheeler, D. J. King and R. L. Garrell, *Lab Chip*, **6**, 199 (2006).
22. A. J. de Mello, M. Habgood, N. L. Lancaster, T. Welton and R. C. R. Wootton, *Lab Chip*, **4**, 417 (2004).
23. N. Dossi, R. Toniolo, A. Pizzariello, E. Carrilho, E. Piccin, S. Battistion and G. Bontempelli, *Lab Chip*, **12**, 153 (2012).
24. T. Hoshino, K. Fujita, A. Higashi, K. Sakiyama, H. Ohno and K. Morishima, *Biochem. Biophys. Res. Commun.*, **427**, 379 (2012).
25. C. S. Effenhauser, G. J. M. Bruln, A. Paulus and M. Ehrat, *Anal. Chem.*, **69**, 3451 (1997).
26. J. S. Wilkes, in Ionic Liquids in Synthesis, Ed. P. Wasserscheid, T. Welton, WILEY-VCH Verlag & Co., KGaA, 1 (2002).
27. W. J. Oldham Jr., in Ionic Liquids: Industrial Applications to Green Chemistry, Ed. R. D. Rogers, K. R. Seddon, Oxford University, Press, 188 (2003).
28. W. Martino, J. F. de la Mora, Y. Yoshida, G. Saito and J. Wilkes, *Green Chem.*, **8**, 390 (2006).
29. C. H. Choi, N. Prasad, N. R. Lee and C. S. Lee, *Biochip J.*, **2**, 27 (2008).
30. B. D. Fitchett, J. B. Rollins and J. C. Conboy, *Langmuir*, **21**, 12179 (2005).
31. E. Lepercq-Bost, M. L. Giorgi, A. Isambert and C. Arnaud, *J. Memb. Sci.*, **314**, 76 (2008).
32. S. van der Graaf, M. L. J. Steegmans, R. G. M. van der Sman, C. G. P. H. Schroen, R. M. Boom, *Colloids Surf., A: Phys. Eng. Aspects*, **266**, 106 (2005).